



ORNL/TM-11029

OAK RIDGE  
NATIONAL  
LABORATORY

MARTIN MARIETTA

High-Temperature Corrosion of  
Metallic Alloys in an Oxidizing  
Atmosphere Containing NaCl

J. I. Federer

OAK RIDGE NATIONAL LABORATORY  
CENTRAL RESEARCH LIBRARY  
CIRCULATION SECTION  
FORM 1000 (11-75)  
**LIBRARY LOAN COPY**  
DO NOT TRANSFER TO ANOTHER PERSON  
If you wish someone else to see this  
report, send in name with report and  
the library will arrange a loan.

OPERATED BY  
MARTIN MARIETTA ENERGY SYSTEMS, INC.  
FOR THE UNITED STATES  
DEPARTMENT OF ENERGY

Printed in the United States of America. Available from  
National Technical Information Service  
U.S. Department of Commerce  
5285 Port Royal Road, Springfield, Virginia 22161  
NTIS price codes---Printed Copy: A03 Microfiche A01

This report was prepared as an account of work sponsored by an agency of the United States Government. Neither the United States Government nor any agency thereof, nor any of their employees, makes any warranty, express or implied, or assumes any legal liability or responsibility for the accuracy, completeness, or usefulness of any information, apparatus, product, or process disclosed, or represents that its use would not infringe privately owned rights. Reference herein to any specific commercial product, process, or service by trade name, trademark, manufacturer, or otherwise, does not necessarily constitute or imply its endorsement, recommendation, or favoring by the United States Government or any agency thereof. The views and opinions of authors expressed herein do not necessarily state or reflect those of the United States Government or any agency thereof.

Metals And Ceramics Division

HIGH-TEMPERATURE CORROSION OF METALLIC ALLOYS  
IN AN OXIDIZING ATMOSPHERE CONTAINING NaCl

J. I. Federer

Date Published - February 1989

Prepared for the  
Assistant Secretary for  
Conservation and Renewable Energy,  
Office of Industrial Programs,  
Waste Energy Recovery Program  
ED 01 01 00 0

NOTICE: This document contains information of a preliminary nature. It is subject to revision or correction and therefore does not represent a final report

Prepared by the  
OAK RIDGE NATIONAL LABORATORY  
Oak Ridge, Tennessee 37831-6285  
operated by  
MARTIN MARIETTA ENERGY SYSTEMS, INC.  
for the  
U.S. DEPARTMENT OF ENERGY  
under Contract DE-AC05-84OR21400



3 4456 0290388 3



## CONTENTS

|                                  |     |
|----------------------------------|-----|
| LIST OF TABLES . . . . .         | v   |
| LIST OF FIGURES . . . . .        | vii |
| ABSTRACT . . . . .               | 1   |
| INTRODUCTION . . . . .           | 1   |
| ALLOYS TESTED . . . . .          | 3   |
| EXPERIMENTAL PROCEDURE . . . . . | 3   |
| RESULTS . . . . .                | 5   |
| WEIGHT CHANGES . . . . .         | 5   |
| DEPTH OF CORROSION . . . . .     | 6   |
| DISCUSSION . . . . .             | 20  |
| ACKNOWLEDGMENTS . . . . .        | 25  |
| REFERENCES . . . . .             | 25  |



## LIST OF TABLES

|          |  |    |
|----------|--|----|
| Table 1. | Alloys used in high-temperature corrosion test . . . . .                               | 4  |
| Table 2. | Atmospheres for corrosion testing of metallic alloys<br>at 1000°C for 1000 h . . . . . | 4  |
| Table 3. | Weight changes in alloys . . . . .   | 6  |
| Table 4. | Depth of corrosion in alloys . . . . .   | 8  |
| Table 5. | Characteristics of alloys . . . . .  | 24 |



LIST OF FIGURES

Fig. 1. Measurements required to determine depth of corrosion . . . . . 7

Fig. 2. Depth of corrosion with and without NaCl . . . . . 9

Fig. 3. Microstructure of Incoloy MA-956 exposed for ~1000 h at 1000°C.  
As polished . . . . . 11

Fig. 4. Microstructure of Incoloy 800 exposed for ~1000 h at 1000°C.  
As polished . . . . . 12

Fig. 5. Microstructure of Inconel 625 exposed for ~1000 h at 1000°C.  
As polished . . . . . 13

Fig. 6. Microstructure of Inconel 601 exposed for ~1000 h at 1000°C.  
As polished . . . . . 14

Fig. 7. Microstructure of Alloy 214 exposed for ~1000 h at 1000°C.  
As polished . . . . . 15

Fig. 8. Microstructure of Hastelloy X exposed for ~1000 h at 1000°C.  
As polished . . . . . 16

Fig. 9. Microstructure of Haynes 188 exposed for ~1000 h at 1000°C to  
Atmosphere 1 and for ~600 h to Atmosphere 2. As polished . . . 17

Fig. 10. Microstructure of nickel aluminide IC-50 exposed for ~1000 h  
at 1000°C. As polished . . . . . 18

Fig. 11. Microstructure of nickel aluminide IC-221 exposed for ~1000 h  
at 1000°C. As polished . . . . . 19

Fig. 12. Relative grain sizes of alloys. (a) Alloy 214; (b) IC-221;  
(c) Inconel 601; (d) Inconel 625; (e) Incoloy 800 . . . . . 21



HIGH-TEMPERATURE CORROSION OF METALLIC ALLOYS  
IN AN OXIDIZING ATMOSPHERE CONTAINING NaCl\*

J. I. Federer

ABSTRACT

A particular heat-exchanger application involved metallic alloys exposed to flue gases of an aluminum remelt furnace. Because the flue gases might contain NaCl and other halides, the corrosion behavior of the alloys was to be investigated. Planned direct exposure of candidate alloys to the flue gases, however, was not conducted because of premature termination of the project. Complementary laboratory testing was conducted on seven commercially available alloys and two nickel aluminides. These materials were exposed to an oxidizing atmosphere containing 0.06 wt % NaCl for 1100 h at 1000°C. Most of the alloys exhibited grain-boundary attack, which resulted in complete oxidation of enveloped grains. The alloys Incoloy MA-956, Incoloy 800, Inconel 625, Inconel 601, Hastelloy X, Haynes 188, and nickel aluminide IC-50 were substantially more corroded than Alloy 214 and nickel aluminide IC-221. The latter two alloys, therefore, would probably be superior to the others in applications involving flue gases containing NaCl. Strength, fabricability, and weldability, which are briefly discussed, would also affect selection of materials.

---

INTRODUCTION

Heat-exchanger systems sponsored by the U.S. Department of Energy in recent years have used both ceramic and metallic materials. The recuperator systems developed and tested by Babcock & Wilcox and by AiResearch Manufacturing Company each had ceramic tube recuperators in series with metallic alloy plate-fin recuperators.<sup>1,2</sup> The fluidized-bed heat exchanger developed and tested by Aerojet Energy Conversion Company used metallic alloys for the distributor plate, steam tubes, containment walls, and distributor plate cleaning apparatus.<sup>3</sup> The raining-bed heat exchanger concept

---

\*Research sponsored by the Waste Energy Recovery Program, Office of Industrial Programs, U.S. Department of Energy, under contract DE-AC05-84OR21400 with Martin Marietta Energy Systems, Inc.

developed by Tecogen, Inc., used metallic alloys for many critical components.<sup>4</sup> During normal operation, the metallic components in these applications will be contacted by flue gases at temperatures up to  $\sim 1000^{\circ}\text{C}$ . The flue gases of many industrial furnaces contain various corrosive compounds, including alkali halides and sulfates. These compounds are corrosive to some metallic alloys and ceramic materials, the severity of corrosion being a function of flue-gas composition and temperature. Thus, strength and corrosion behavior are important factors in selecting materials for specific applications.

The raining-bed heat exchanger was being developed by Tecogen, Inc., for installation and performance testing on an aluminum remelt furnace at a host industrial site. The project was prematurely terminated because of a labor strike at the host site and because of change of ownership of the host facility. Metallic alloys had been selected for plates, baffles, and structural members of the heat exchanger. The results of earlier studies indicated that some corrosion would occur. Whereas a compact metallic plate-fin recuperator probably could not operate successfully at  $1000^{\circ}\text{C}$  or higher because of oxidation, corrosion, and distortion, the raining bed was designed to be relatively unaffected by the effects of high temperatures through the use of initially thick cross sections and large flue gas passages. Nevertheless, additional information on the corrosion behavior of materials was needed to optimize the design for future applications.

Planned corrosion testing included installation of specimens of various alloys in the heat exchanger for exposure during performance tests. Subsequent retrieval and examination of the specimens would indicate the relative corrosion behavior of the materials. Concurrently, testing was to be conducted in a laboratory furnace to compare the oxidation and corrosion behavior of various alloys under controlled conditions using a single corrosion species. These data were intended to supplement the exposure test in the heat exchanger by indicating the relative susceptibility of the alloys to corrosion and by revealing corrosion modes. Because the project was prematurely terminated, only some of the laboratory testing was done. The results of that work are discussed herein.

Metallic alloys were exposed to oxidizing and corrosive atmospheres at  $1000^{\circ}\text{C}$  in laboratory furnaces. Weight changes and depth and character of

attack were determined. The alloys were then compared for the intended application on the basis of the corrosion results and other available properties.

#### ALLOYS TESTED

The nominal compositions of the alloys are shown in Table 1. Seven commercially available Fe-, Ni-, or Co-based alloys and two recently developed nickel aluminides were used. Most of the alloys contain substantial amounts of Cr for resistance to high-temperature oxidation. Two alloys, Incoloy MA-956 and Alloy 214, contain about 4.5 wt % Al for improved resistance to oxidation. Incoloy MA-956 also contains  $Y_2O_3$  particles for dispersion strengthening. Haynes 188 and Alloy 214 contain La and Y, respectively, for increasing the adherence of oxide films formed during exposure to oxidizing environments. Other elements are included in the alloys to improve high-temperature strength and creep properties.

#### EXPERIMENTAL PROCEDURE

Two sets of specimens measuring about 19 mm by 25 mm were prepared from sheet material of various thickness. The thickness of the specimens was measured with a micrometer caliper at the four corners and the middle to obtain an average value, and the specimens were weighed. The specimens were then placed in an alumina boat in a 6-cm-ID alumina furnace tube for exposure to the flowing atmospheres. The arrangement of specimens in the boat allowed access of the atmosphere to all surfaces. One set of specimens was exposed to Atmosphere 1, the simulated combustion products of  $CH_4$  with 10% excess air (Table 2). This atmosphere was prepared by bubbling metered quantities of air,  $N_2$ , and  $CO_2$  through water at about 65°C. The other set of specimens was exposed to Atmosphere 2, which consisted of  $N_2$ ,  $O_2$ ,  $H_2O$ , and a small concentration (0.06 wt %) of NaCl vapor (Table 2). The NaCl vapor was formed by evaporation from a crucible in the furnace tube. The latter atmosphere was not intended to simulate an actual combustion atmosphere. Instead, the intent of the experiment was to

Table 1. Alloys used in high-temperature corrosion test

| Alloy                      | Nominal composition<br>(wt %) <sup>a</sup> |      |     |                   |      |     |                                   | Source <sup>b</sup> |
|----------------------------|--|------|-----|-------------------|------|-----|-----------------------------------|---------------------|
|                            | Al   | Co   | Cr  | Fe                | Ni   | Ti  | Other                             |                     |
| Incoloy MA-956             | 4.5  |      | 20  | bal. <sup>c</sup> |      | 0.5 | 0.5 Y <sub>2</sub> O <sub>3</sub> | A                   |
| Incoloy 800                | 0.3  |      | 21  | bal.              | 31   | 0.3 |                                   | A                   |
| Inconel 625                | 0.4  | 1    | 22  | 5                 | 58   | 0.4 | 9 Mo, 3.7 Nb+Ta                   | A                   |
| Inconel 601                | 1.3  |      | 23  | 14                | bal. | 0.3 |                                   | A                   |
| Alloy 214                  | 4.5  |      | 16  | 2.5               | bal. |     | Y (present)                       | B                   |
| Hastelloy X                |  | 1.8  | 22  | 19                | bal. |     | 9 Mo, 0.5 W                       | B                   |
| Haynes 188                 |  | bal. | 22  | 3                 | 22   |     | 15 W, 0.1 La                      | B                   |
| Nickel aluminide<br>IC-50  | 11.3                                       |      |     |                   | bal. |     | 0.02 B, 0.6 Zr                    | C                   |
| Nickel aluminide<br>IC-221 | 8.5  |      | 7.8 |                   | bal. |     | 0.02 B, 1.7 Zr                    | C                   |

<sup>a</sup>These alloys typically contain small amounts of C, Mn, P, S, and Si.

<sup>b</sup>A - Huntington Alloys, Inc.; B - Cabot Corp.; C - ORNL.

<sup>c</sup>Balance.

Table 2. Atmospheres for corrosion testing of metallic alloys at 1000°C for 1000 h

| Component        | Atmosphere 1 -<br>synthetic combustion products<br>of CH <sub>4</sub> with excess air <sup>a</sup> |      | Atmosphere 2 -<br>oxidizing atmosphere<br>containing NaCl vapor <sup>b</sup> |      |
|------------------|--|------|--|------|
|                  | vol %  | wt % | vol %  | wt % |
| N <sub>2</sub>   | 73.9   | 74.3 | 64.9   | 67.9 |
| O <sub>2</sub>   | 1.7  | 2.1  | 16.2   | 19.4 |
| CO <sub>2</sub>  | 8.4  | 13.3 | 0  | 0    |
| H <sub>2</sub> O | 16.0   | 10.3 | 18.9   | 12.7 |
| NaCl             | 0  | 0    | 0.02   | 0.06 |

<sup>a</sup>~3000 cm<sup>3</sup>/min in 6-cm-ID furnace tube.

<sup>b</sup>~8500 cm<sup>3</sup>/min during first 500 h, ~1500 cm<sup>3</sup>/min during next 500 h, in 6-cm-ID furnace tube.

provide an oxidizing atmosphere in which the effect of a small concentration of NaCl on the relative oxidation behavior of the alloys could be assessed.

Specimens were exposed to each atmosphere for about 1000 h at 1000°C and 100 kPa. Weight changes were determined after about 500 and 1000 h. Specimens were brushed with a bristle brush to remove loose scale, then weighed. After the final exposures, specimens were sectioned for metallographic examination and then oxidation or corrosion depths were measured microscopically.

## RESULTS

### WEIGHT CHANGES

All specimens had visible oxide layers. Alloy 214 appeared to have been least affected by either atmosphere. Specimens changed from a metallic luster to medium gray or black, except for nickel aluminide IC-50, which had a green surface. Weight changes were caused by formation of partially or completely adherent oxide layers. Oxidation of Co, Cr, Fe, and Ni causes weight increases of about 27 to 46%, depending on the particular oxide formed. Completely adherent layers, therefore, would cause a weight increase. The alloys, however, have significantly higher thermal coefficients of expansion than the individual metal oxides ( $\text{Cr}_2\text{O}_3$ ,  $\text{Fe}_2\text{O}_3$ , etc.) and probably have higher thermal coefficients than the complex oxides that form during oxidation of the alloys. During cooling from 1000°C, the metal-oxide interface is highly stressed, which causes detachment (spalling) of part of the oxide. Depending on the amount of spalling, the net weight can either increase or decrease. In addition, the volatility of oxides of Mo and W, which are present in several alloys, might affect the weights.

Weight changes occurring in Atmospheres 1 and 2 are shown in Table 3. The weight-change rates are based on the initial surface areas and the exposure times. The results show that weight changes were generally higher in Atmosphere 2, which contained NaCl vapor, than in Atmosphere 1, except for Alloy 214 and nickel aluminide IC-221. As previously mentioned,

Table 3. Weight changes in alloys

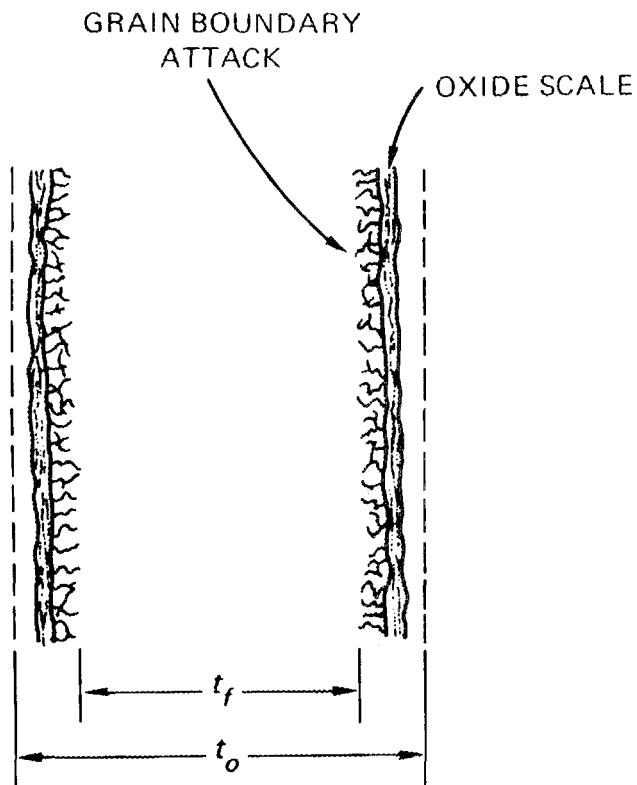
| Alloy                      | Cumulative weight change rate<br>( $\mu\text{g}/\text{mm}^2 \cdot \text{s}$ ) |        |              |          |
|----------------------------|---|--------|--------------|----------|
|                            | Atmosphere 1  |        | Atmosphere 2 |          |
|                            | 500 h   | 1000 h | 600 h        | 1100 h   |
| Incoloy MA-956             | +4  | +4     | +41          | +236     |
| Incoloy 800                | -29   | -67    | -405         | -523     |
| Inconel 625                | -1  | -4     | +77          | -448     |
| Inconel 601                | +9  | +11    | -221         | -106     |
| Alloy 214                  | +5  | +4     | +1           | +1       |
| Hastelloy X                | -14   | -23    | +131         | +56      |
| Haynes 188                 | +5  | +5     | <i>a</i>     | <i>a</i> |
| Nickel aluminide<br>IC-50  | +6  | +8     | +197         | +277     |
| Nickel aluminide<br>IC-221 | +14   | +17    | +18          | +8       |

<sup>a</sup>Not determined because of extensive reaction with ceramic support.

however, the weight changes are strongly dependent on spalling. Although the weight changes indicate the relative corrosion behavior of the alloys, the depth of corrosion, discussed in the next section, is a more accurate indicator.

#### DEPTH OF CORROSION

The depth of corrosion was determined by comparing the original thickness with the thickness of uncorroded material. The measurements required to determine this value are illustrated in Fig. 1. The original thickness ( $t_o$ ) was measured with a micrometer caliper at the four corners and center of the specimens. After exposure, a sample was mounted and polished so that a section perpendicular to the two major surfaces could be examined. The thickness of uncorroded material ( $t_f$ ) was determined at five locations within the section by measuring from the deepest grain-boundary penetration on one side to the deepest penetration on the opposite side.



$t_o$  = ORIGINAL THICKNESS

$t_f$  = THICKNESS OF UNCORRODED MATERIAL

$\frac{t_o - t_f}{2}$  = MEAN DEPTH OF CORROSION

Fig. 1. Measurements required to determine depth of corrosion.

If there was no grain-boundary attack, measurements were made at the metal-oxide interface. The average  $t_o$  and  $t_f$  measurements were then used to calculate the mean depth of corrosion.

The depth of corrosion was greater in Atmosphere 2 than in Atmosphere 1, although only slightly greater for Alloy 214 and nickel aluminide IC-221, as shown in Table 4. The results in Table 4 show that the depth of corrosion (oxidation) in Atmosphere 1 was about the same after 500 and 1000 h, implying that the oxide layers were protective. In

Table 4. Depth of corrosion in alloys

| Alloy                      | Depth of corrosion<br>(mm) |        |              |                   |
|----------------------------|----------------------------|--------|--------------|-------------------|
|                            | Atmosphere 1               |        | Atmosphere 2 |                   |
|                            | 500 h                      | 1000 h | 600 h        | 1100 h            |
| Incoloy MA-956             | 0.01                       | 0.05   | 0.03         | 0.51              |
| Incoloy 800                | 0.29                       | 0.28   | 0.24         | 0.55              |
| Inconel 625                | 0.03                       | 0.04   | 0.31         | 0.45              |
| Inconel 601                | 0.08                       | 0.06   | 0.24         | 0.36              |
| Alloy 214                  | 0.01                       | 0      | 0.03         | 0.04              |
| Hastelloy X                | 0.01                       | 0.01   | 0.12         | 0.27 <sup>a</sup> |
| Haynes 188                 | 0                          | 0.03   | 0.64         | <i>b</i>          |
| Nickel aluminide<br>IC-50  | 0.06                       | 0.06   | 0.07         | 0.37 <sup>a</sup> |
| Nickel aluminide<br>IC-221 | 0.10                       | 0.09   | 0.03         | 0.10              |

<sup>a</sup>Total thickness.

<sup>b</sup>Not determined because of extensive reaction with ceramic support.

Atmosphere 2, however, several alloys exhibited increasing attack with increasing exposure time, implying that the oxide layers were not protective. The behavior of Incoloy MA-956 was anomalous in that part of the specimen corroded to a depth of only about 0.1 mm but to about 0.5 mm in other regions. As will be shown, the oxidation or corrosion caused formation of oxide layers and grain-boundary attack.

The depth of corrosion does not necessarily correlate with weight changes (Table 3) because of spalling of the oxide layers. Two alloys could have the same depth of corrosion but exhibit greatly different weight changes. In both cases, the same amount of material is oxidized or corroded but the net weight change depends on the adherence of the oxide layers, as previously discussed.

The depth of corrosion for the alloys is illustrated in Fig. 2. Two materials, Alloy 214 and nickel aluminide IC-221, exhibited significantly less corrosion than the others. As a reference point, a depth of corrosion of 0.1 mm in 1000 h extrapolates linearly to about 0.9 mm/year (~0.035 in./year). Alloy 214 and IC-221 had corrosion depths of 0.1 mm or

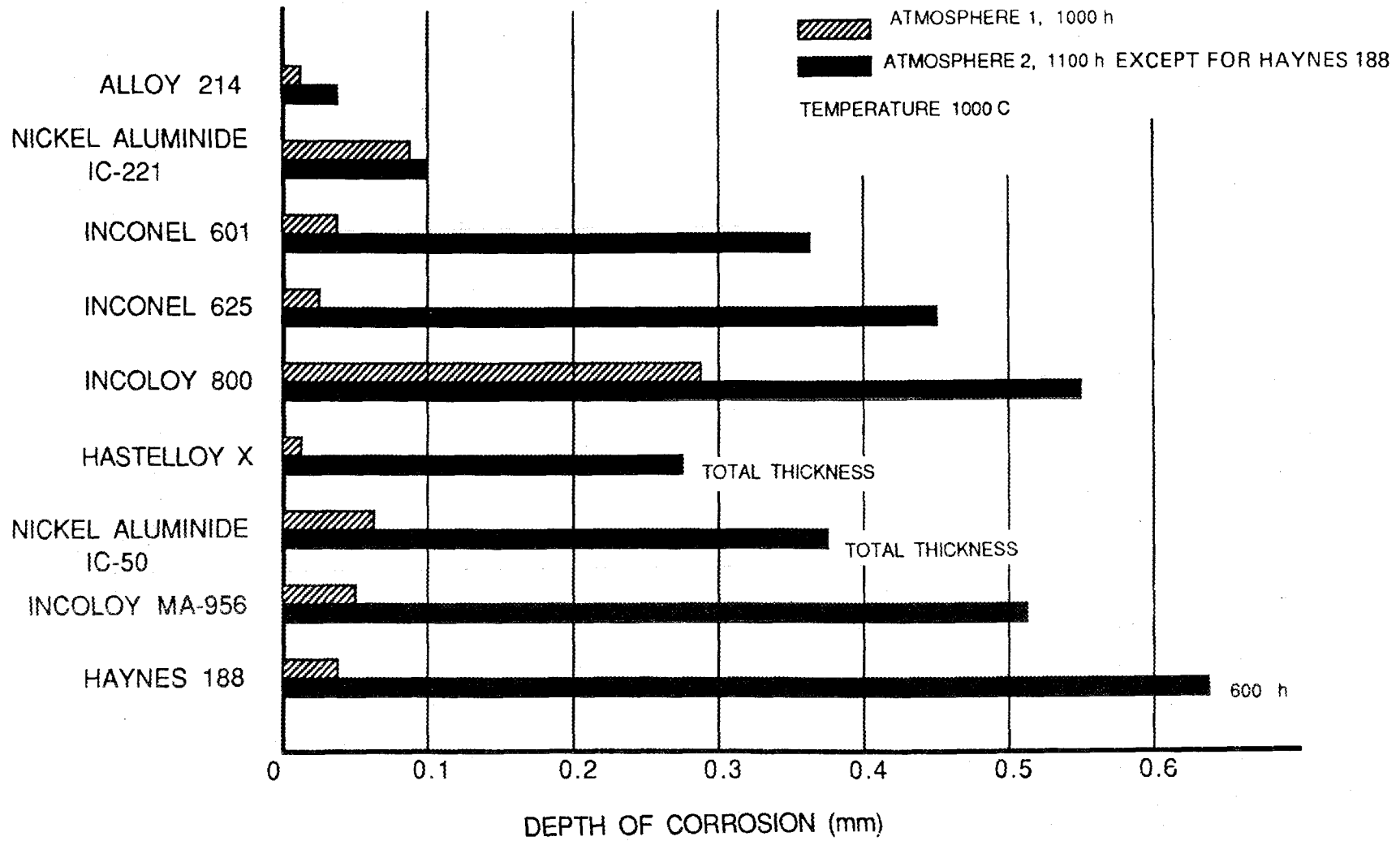


Fig. 2. Depth of corrosion with and without NaCl.

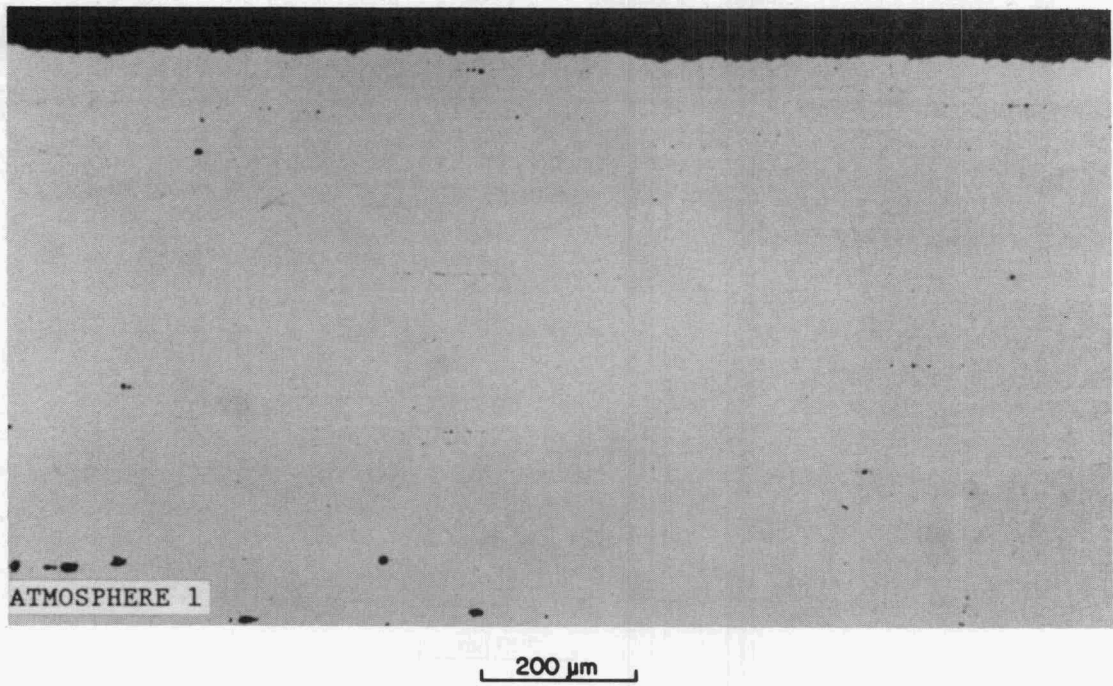
less in 1000 h, whereas the other alloys had corrosion depths of about 0.3 mm or more.

These corrosion results are presented for the purpose of comparison and do not necessarily represent those that would occur in an industrial furnace environment containing NaCl. Corrosion rates of approximately the same magnitude, however, have occurred in some of the same alloys when exposed to flue gases at 1000 to 1100°C in an aluminum remelt furnace.<sup>5</sup> Uncoated Inconel 625 and Alloy 214 had a corrosion rate of 2.8 mm/year, and Inconel 601 coated with Al had a rate of 5.2 mm/year. On the other hand, Haynes 188 coated with Al had a corrosion rate of only 0.9 mm/year, which is much lower than that occurring in Haynes 188 in the current work. The results of the current work, which reveal differences in corrosion behavior among the various alloys, should be considered along with other factors, such as mechanical strength and fabricability, in selecting materials for specific applications.

Microstructures of materials exposed to both atmospheres in Figs. 3 through 11 reveal three effects of oxidation or corrosion: formation of an oxide layer, subsurface oxidation, and grain-boundary attack. Formation of an oxide layer might cause less concern than the other two types of corrosion. Uniform oxidation, such as that exhibited by Incoloy MA-956 exposed to Atmosphere 1, causes gradual surface recession of the material. The load-bearing cross section of a material experiencing this type of surface recession would decrease with time at a predictable rate. Corrosion by subsurface oxidation and grain-boundary attack, however, occurs ahead of the receding surface. The effective load-bearing cross section, therefore, would be less than that indicated by surface dimensions. Stress concentrations associated with the localized corrosion of subsurface oxidation and grain-boundary attack would probably accelerate failure of the material, much as that caused by stress-corrosion in aqueous environments.

Figures 3 through 11 show that one or more of the three types of corrosion was generally more severe in Atmosphere 2. Incoloy MA-956, for example, oxidized very little in Atmosphere 1 but corroded extensively in Atmosphere 2 (Fig. 3). Incoloy 800 oxidized or corroded extensively in both atmospheres (Fig. 4). Inconel 625 had subsurface oxidation in

Y211210



Y211217

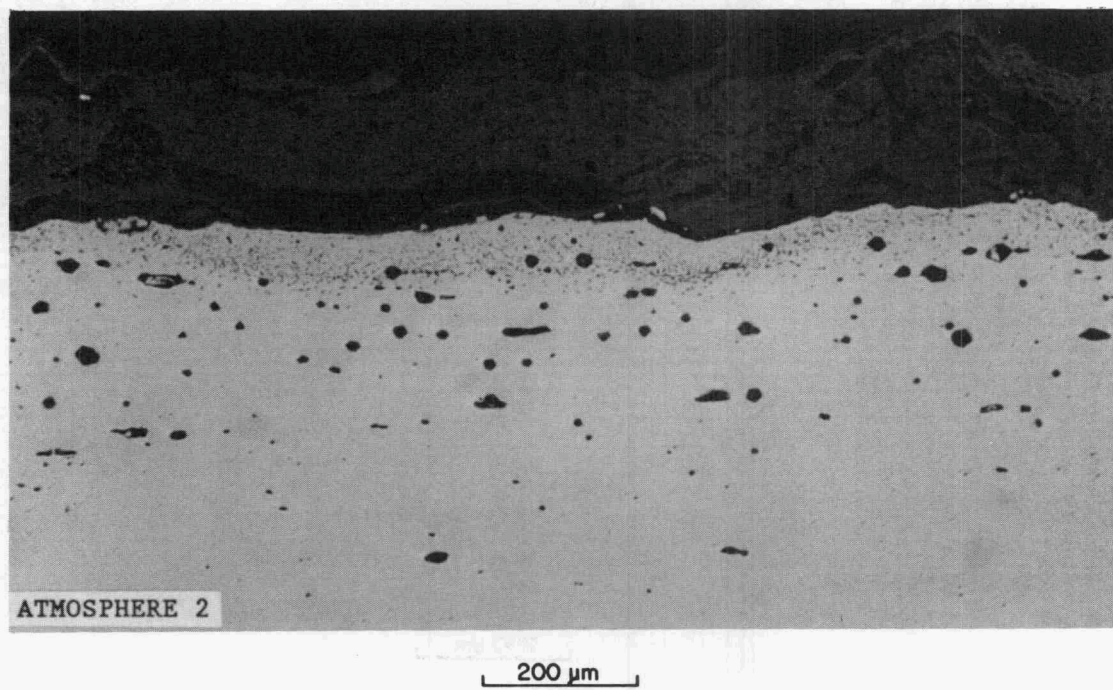
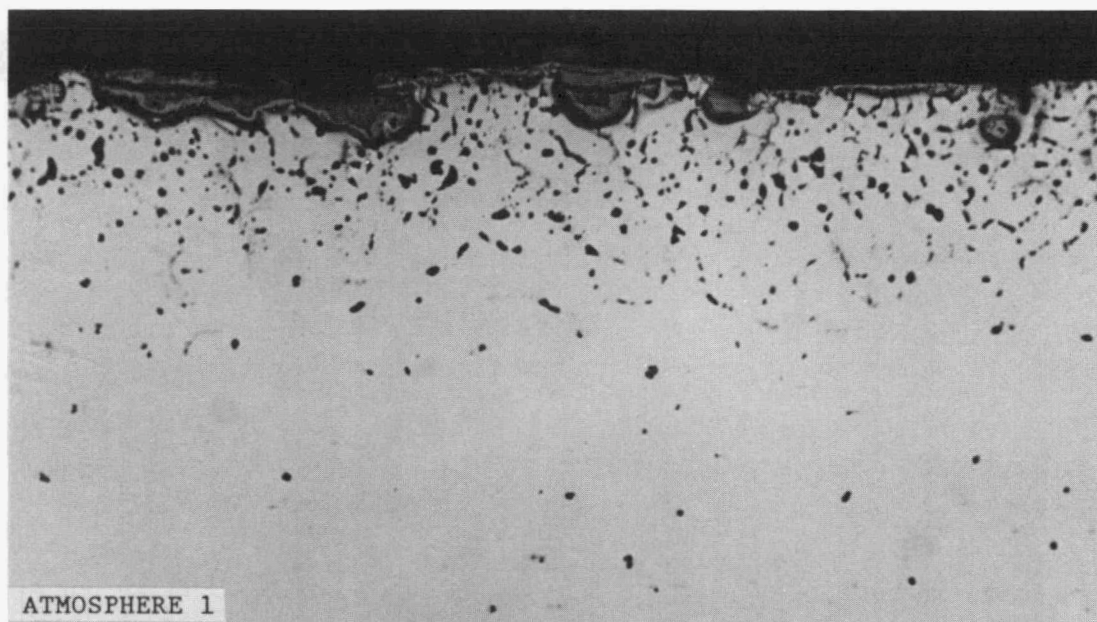


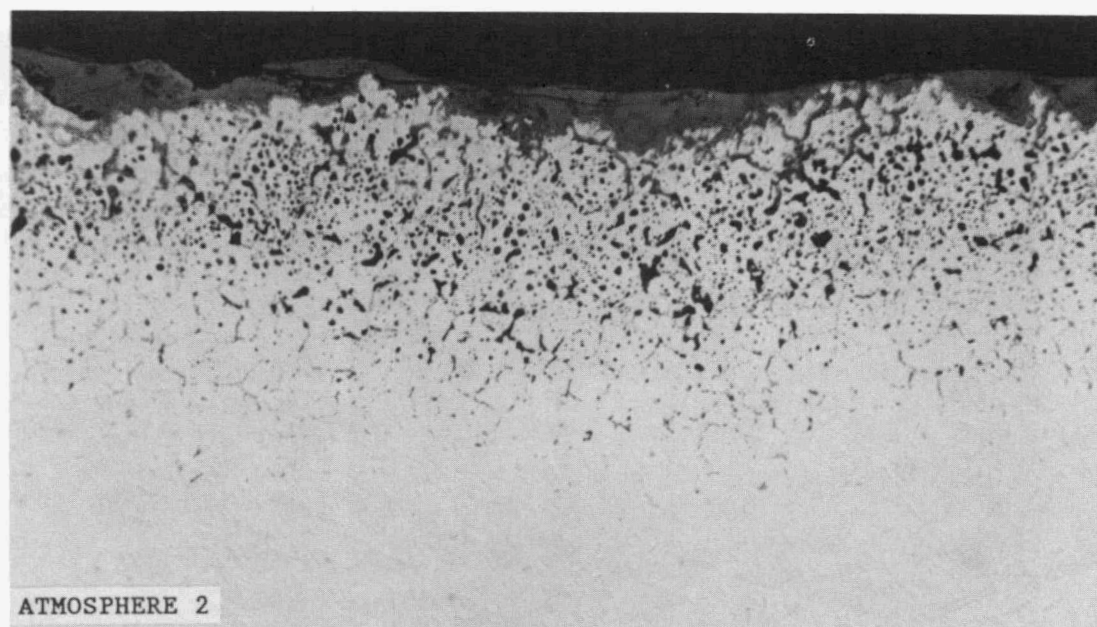
Fig. 3. Microstructure of Incoloy MA-956 exposed for ~1000 h at 1000°C. As polished.

Y211208



200 μm

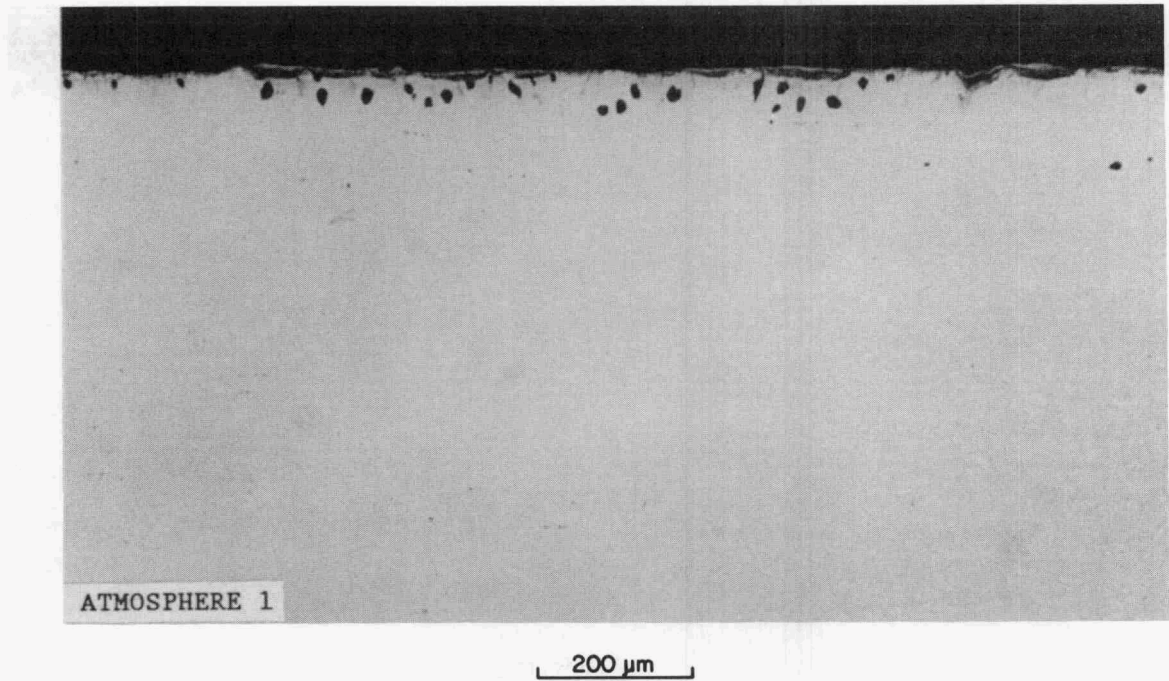
Y211219



200 μm

Fig. 4. Microstructure of Incoloy 800 exposed for ~1000 h at 1000°C. As polished.

Y211211



Y211220

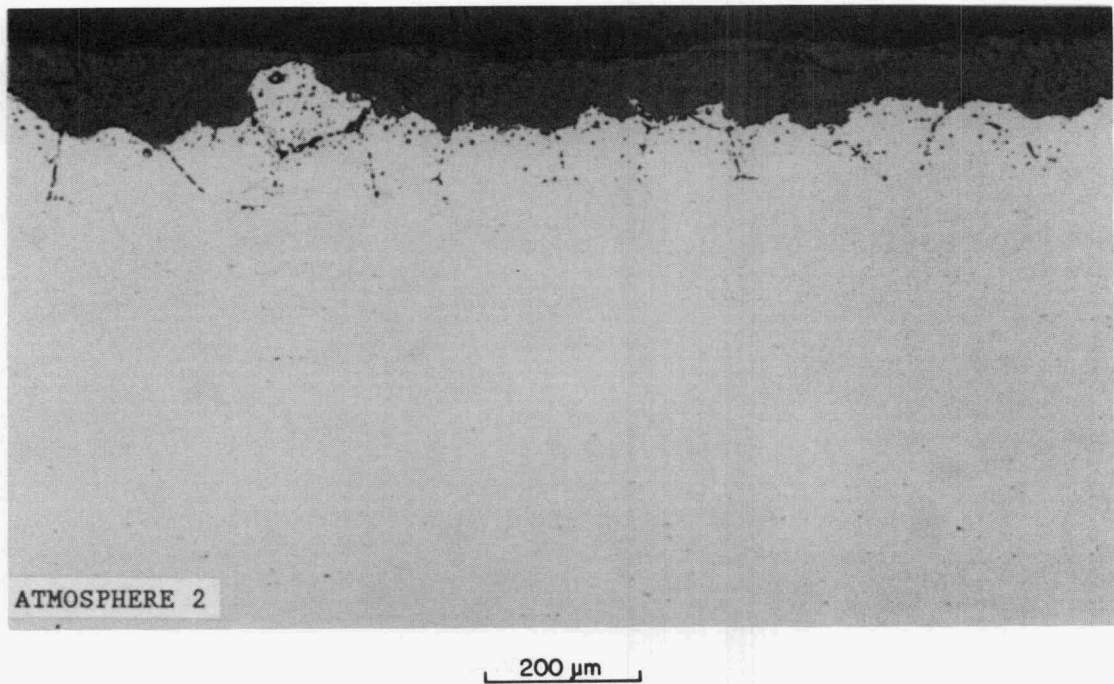
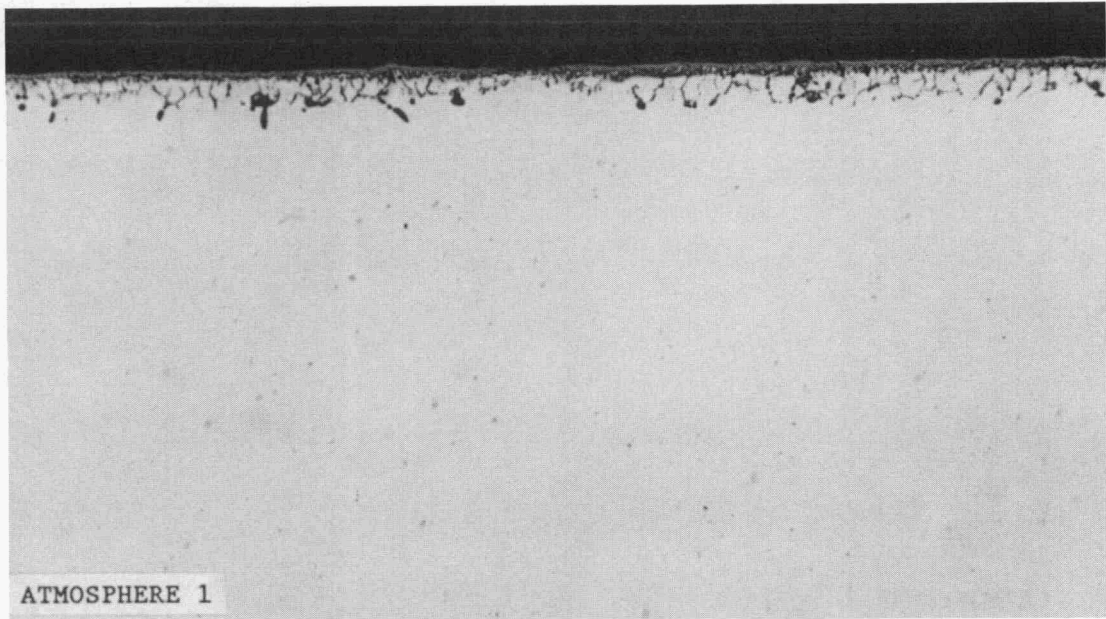


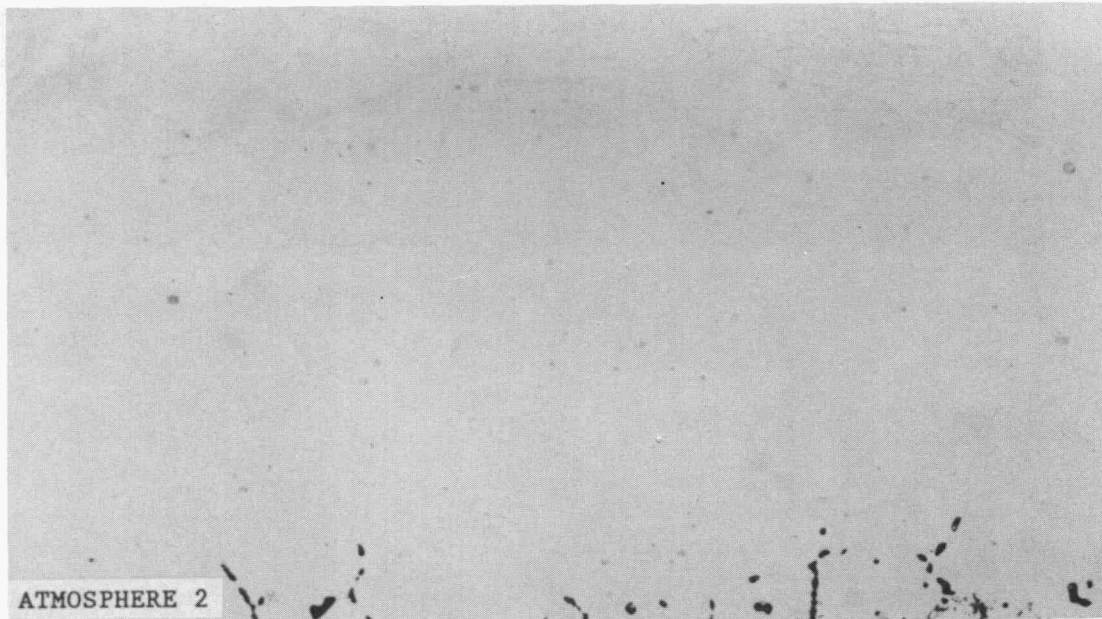
Fig. 5. Microstructure of Inconel 625 exposed for ~1000 h at 1000°C. As polished.

Y211213



200 μm

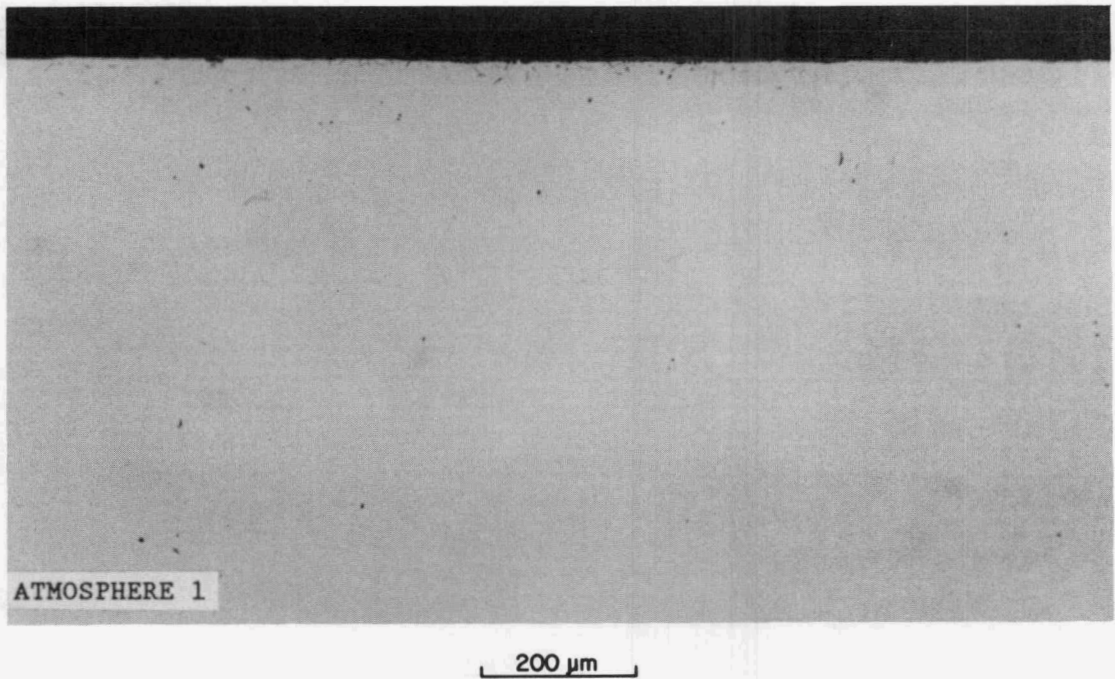
Y211221



200 μm

Fig. 6. Microstructure of Inconel 601 exposed for ~1000 h at 1000°C. As polished.

Y211214



Y211222

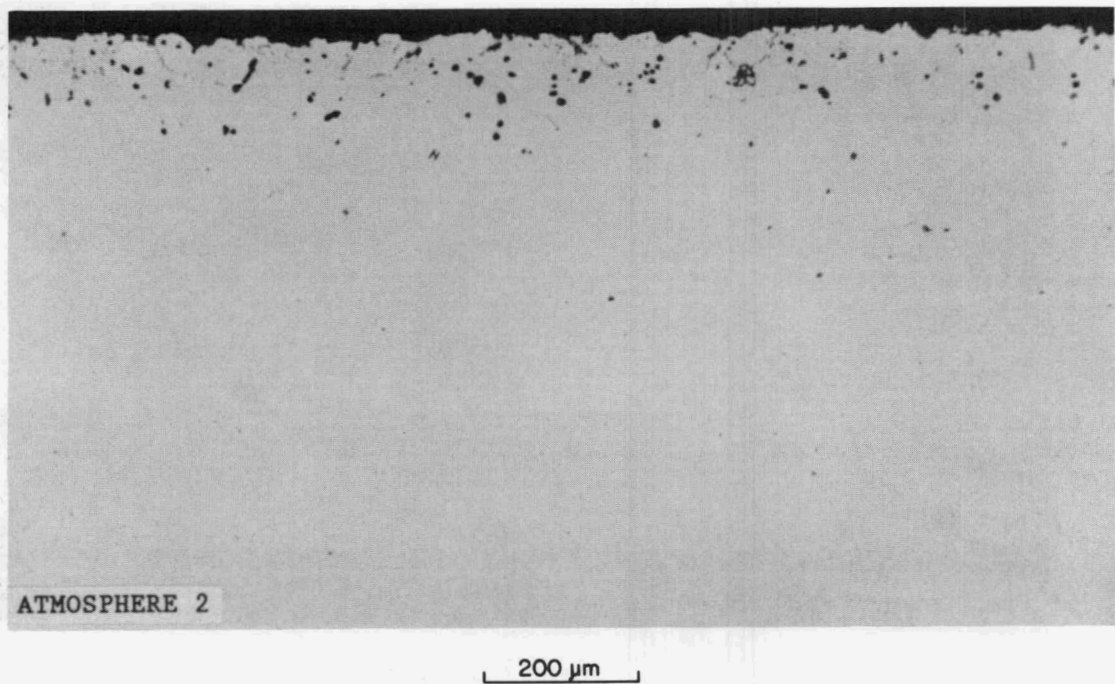
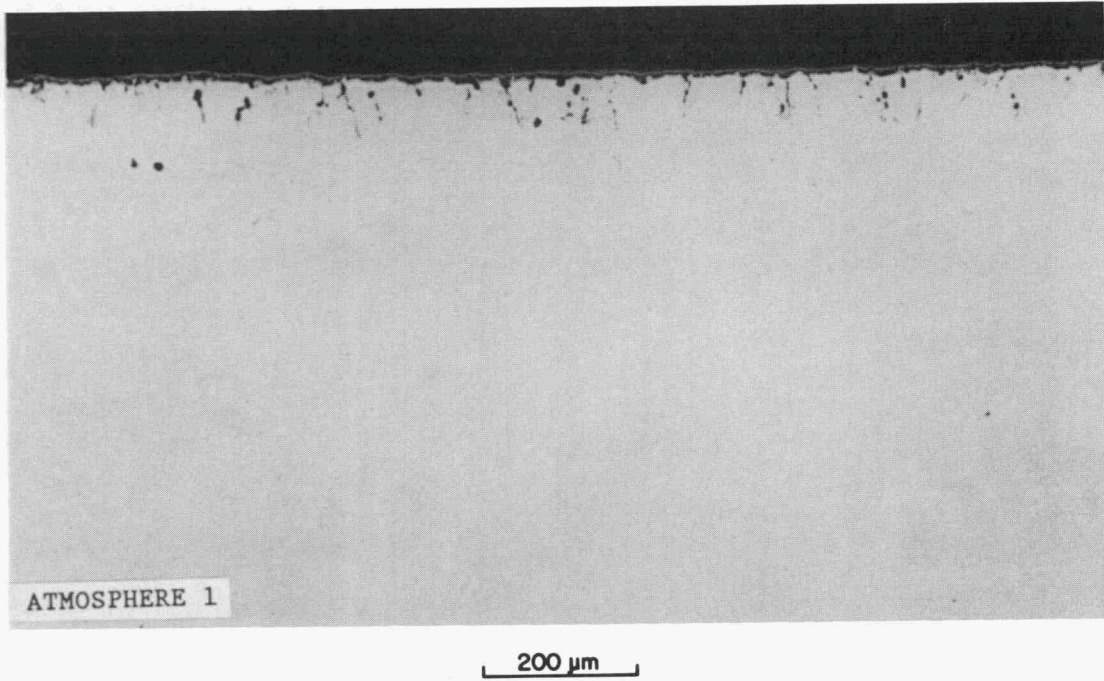


Fig. 7. Microstructure of Alloy 214 exposed for ~1000 h at 1000°C. As polished.

Y211209



Y211223

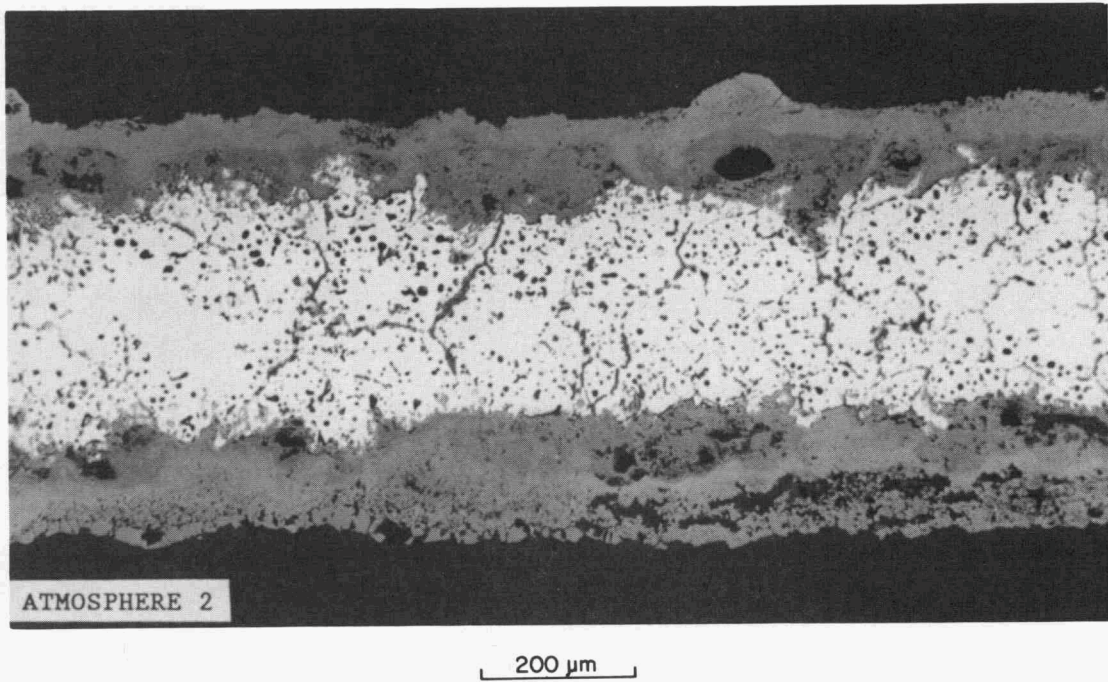
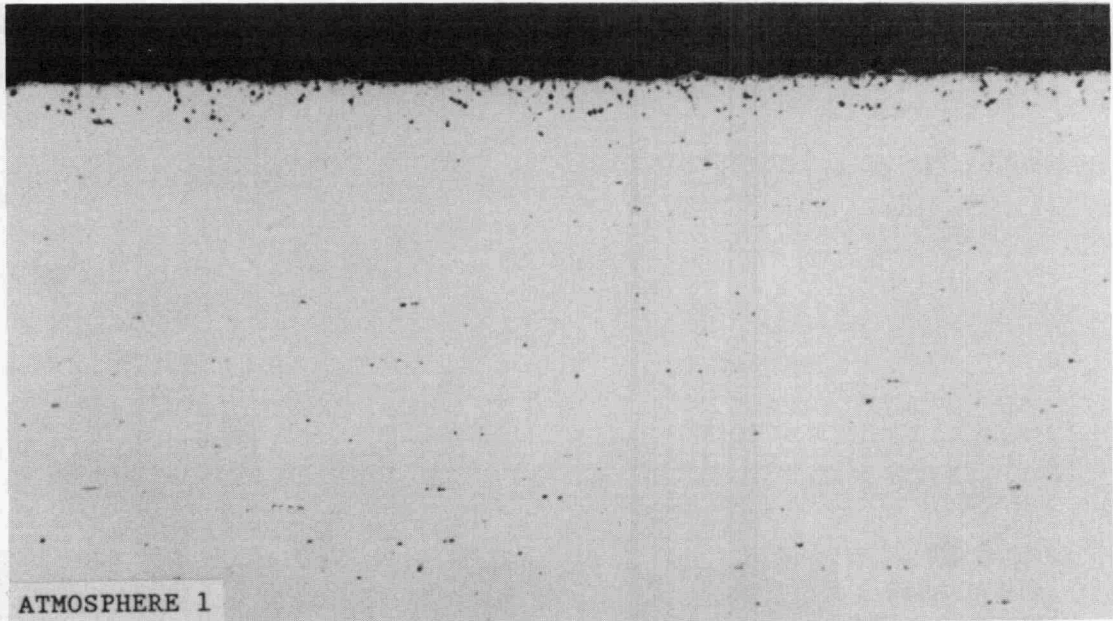


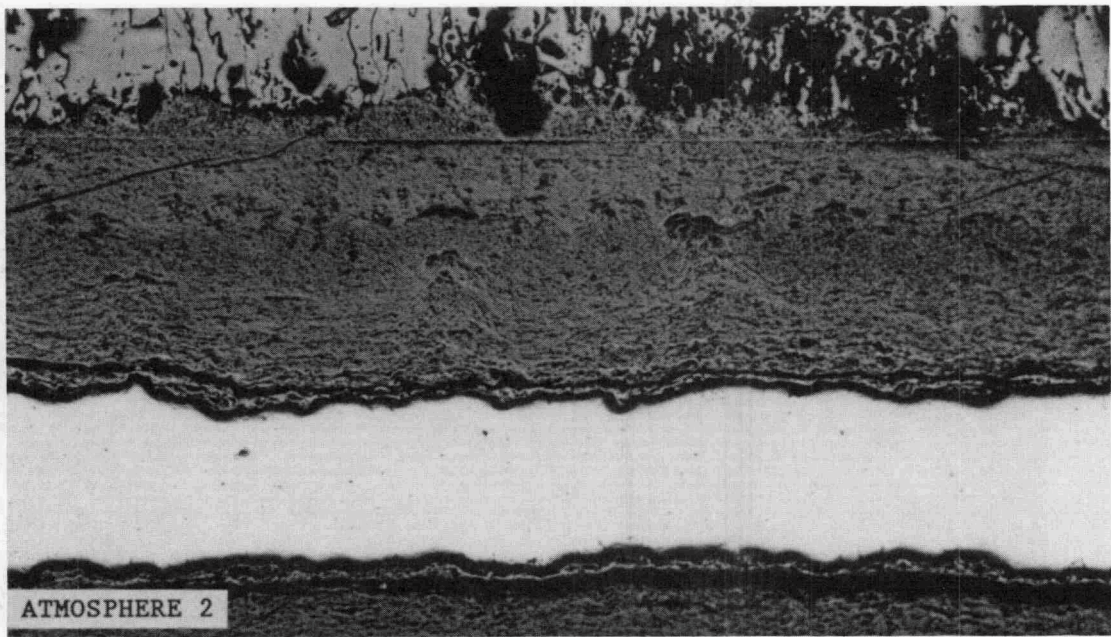
Fig. 8. Microstructure of Hastelloy X exposed for ~1000 h at 1000°C. As polished.

Y211212



200  $\mu\text{m}$

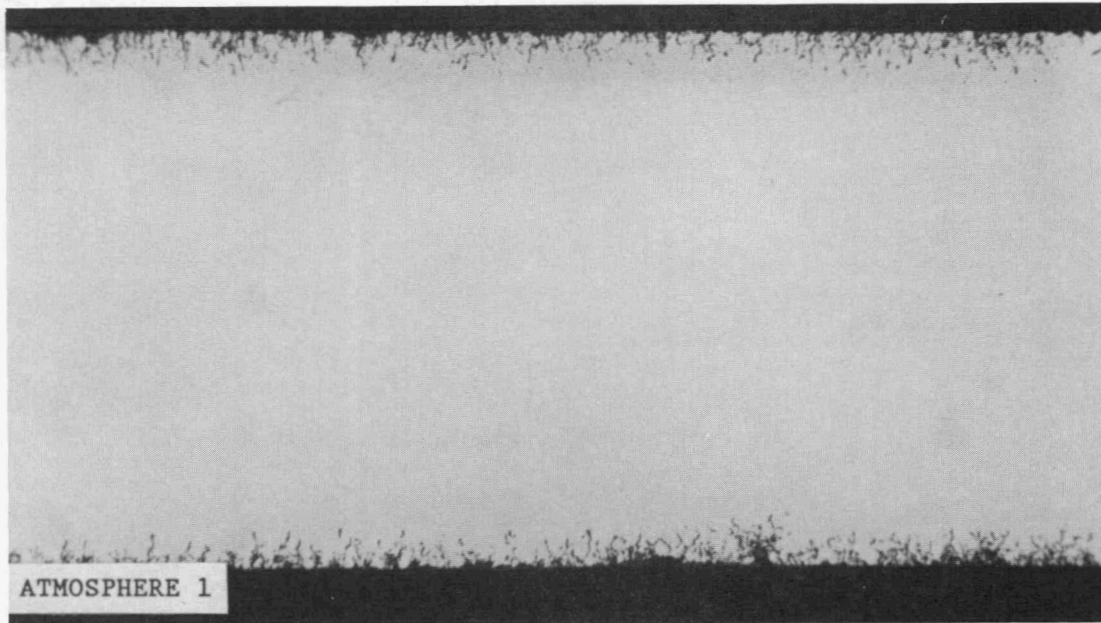
Y211421



400  $\mu\text{m}$

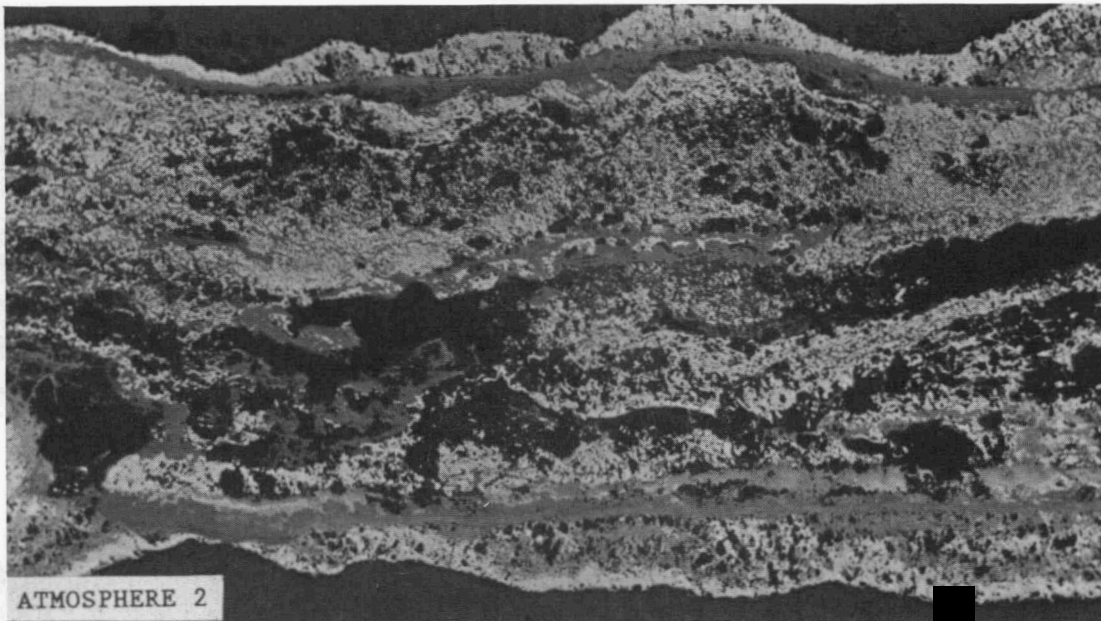
Fig. 9. Microstructure of Haynes 188 exposed for ~1000 h at 1000°C to Atmosphere 1 and for ~600 h to Atmosphere 2. As polished.

Y211205



200 μm

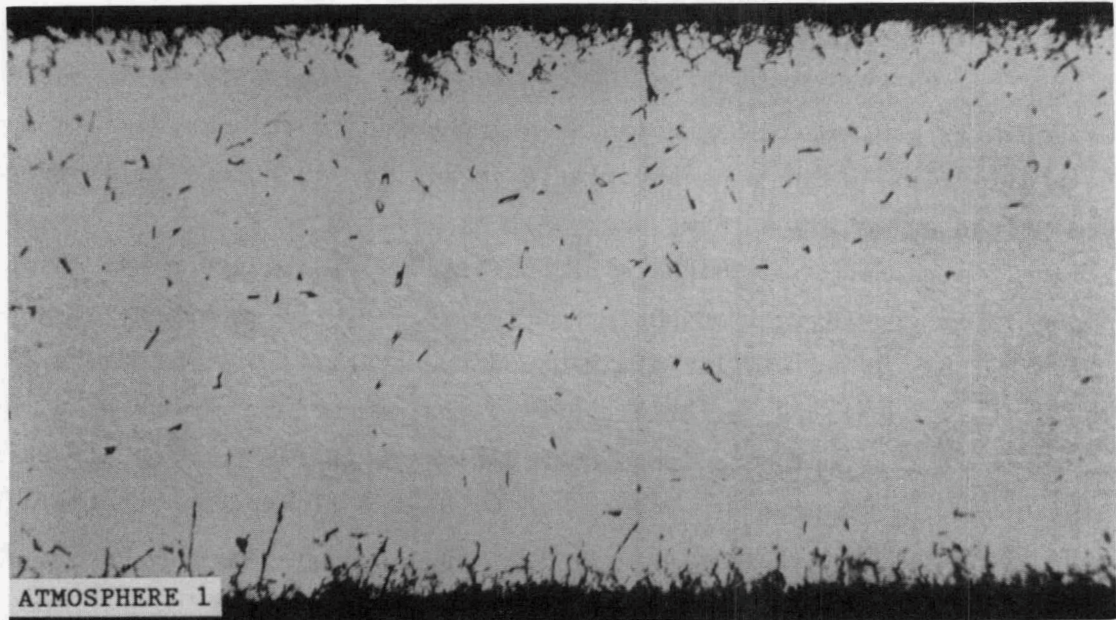
Y211224



400 μm

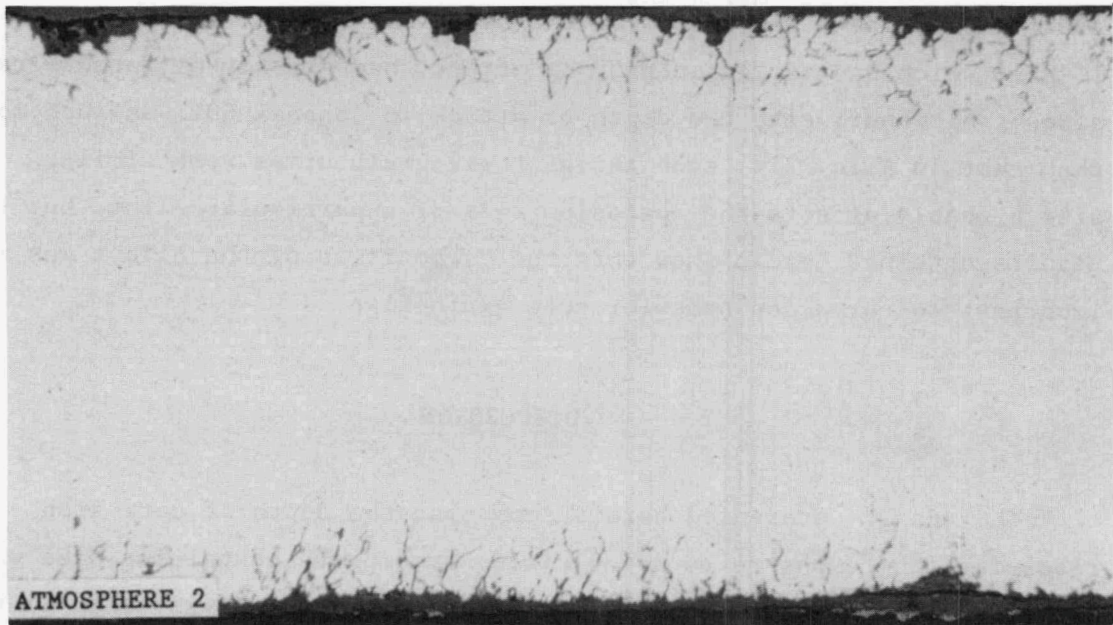
Fig. 10. Microstructure of nickel aluminide IC-50 exposed for ~1000 h at 1000°C. As polished.

Y211206



200 μm

Y211225



200 μm

Fig. 11. Microstructure of nickel aluminide IC-221 exposed for ~1000 h at 1000°C. As polished.

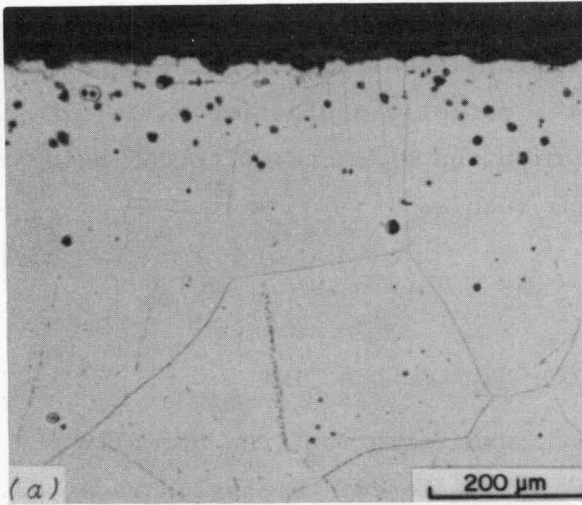
Atmosphere 1, but grain-boundary attack is more apparent in Atmosphere 2 (Fig. 5). Inconel 601 had more extensive grain-boundary attack in Atmosphere 2 (Fig. 6), whereas Hastelloy X and nickel aluminide IC-50 were essentially completely destroyed by grain-boundary attack (Figs. 8 and 10). Even Alloy 214, which had very little attack in Atmosphere 1, exhibited subsurface oxidation in Atmosphere 2 (Fig. 7). Haynes 188, which was only slightly attacked in Atmosphere 1, exhibited severe surface recession and oxide-layer growth in Atmosphere 2 (Fig. 9). Nickel aluminide IC-221, on the other hand, had similar grain-boundary attack in both atmospheres (Fig. 11). Generally, materials having grain-boundary attack as a result of exposure to Atmosphere 1 had more extensive grain-boundary attack during exposure to Atmosphere 2. Figures 4, 6, 8, and 11 indicate that grain-boundary attack envelope grains near the surface. The grain boundary region expands into the grains, gradually converting grains into the oxide surface layer.

The possibility that the depth of attack was related to grain size was investigated. Microstructures of several alloys in Fig. 12 reveal that grain size alone did not control the depth of attack. Alloy 214 and IC-221, which had similar depths of attack, had greatly different grain sizes. Alternatively, the depth of attack in Inconel 601 was much more than that in Alloy 214, even though their grain sizes were similar. Grain size probably affects the corrosion rate of a particular alloy, but the results obtained herein show that the composition of the alloys was more important to corrosion behavior than grain size.

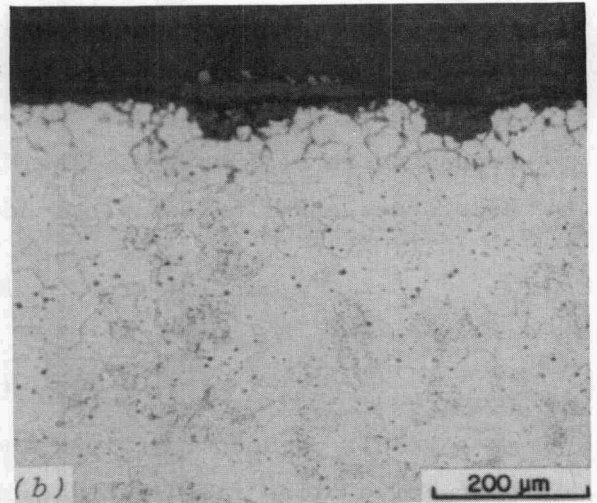
## DISCUSSION

The results presented herein show that the depth of corrosion resulting from exposure to an oxidizing atmosphere containing NaCl was substantially less in Alloy 214 and nickel aluminide IC-221 than in the other materials. Alloy 214 and IC-221 are both Ni-base alloys containing substantial amounts of Cr and Al. The other, less resistant materials include two Fe-base alloys (Incoloy MA-956 and Incoloy 800), three Ni-base

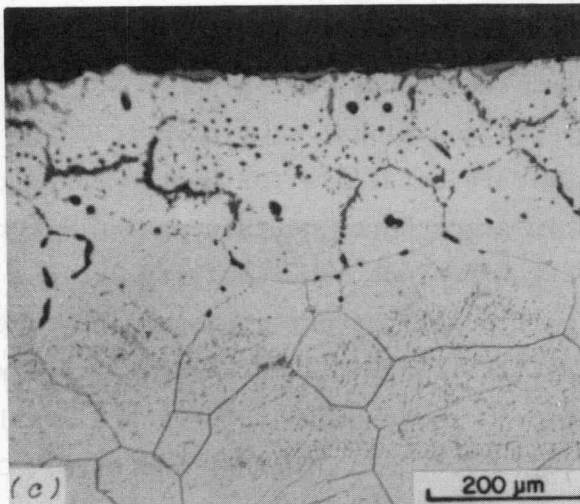
Y212301



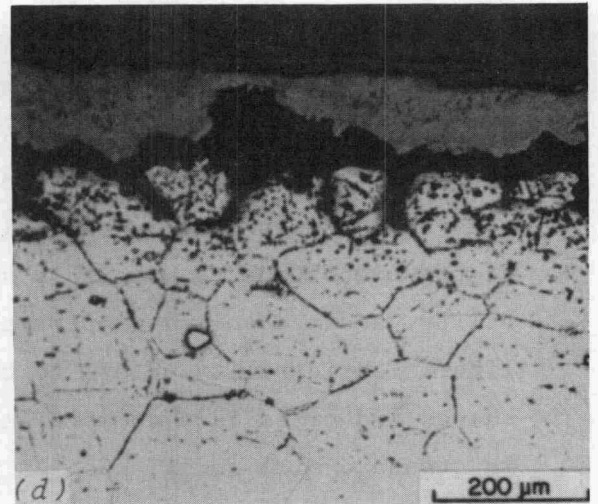
Y212302



Y212300



Y212299



Y212298

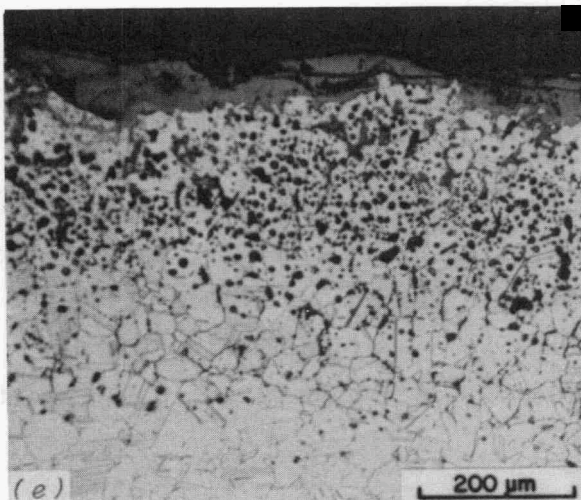
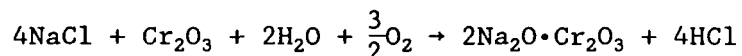
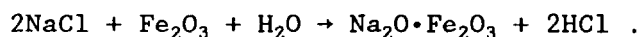


Fig. 12. Relative grain sizes of alloys. (a) Alloy 214; (b) IC-221; (c) Inconel 601; (d) Inconel 625; (e) Incoloy 800.

alloys containing refractory metals (Inconel 625, Inconel 601, and Hastelloy X), a Co-base alloy (Haynes 188), and nickel aluminide IC-50, containing no Cr. Although the corrosion mechanism was not determined in this study, chemical alteration of the normally protective oxide film is suspected to be involved. The NaCl might have reacted with the oxide film to produce other oxides via reactions such as



and



As a result of such reactions and compound formation, the normally protective oxide film might be chemically altered. Diffusion rates of metals and oxygen in the oxide film might be enhanced, which would cause a greater amount of oxidation and larger weight changes. These reactions would be similar to those occurring in the  $\text{SiO}_2$  film on SiC exposed to oxidizing atmospheres containing alkali compounds.<sup>6</sup>

The corrosion behavior of Alloy 214 and nickel aluminide IC-221 suggests that the two alloys are candidate materials for heat exchanger and other high-temperature applications in atmospheres containing NaCl. Other factors important to materials selection include fabricability, weldability, and mechanical properties, particularly creep strength and rupture life. Fabricability refers to the availability of a material in required shapes and sizes from commercial vendors. Most of the alloys are available in standard mill forms, such as plate, sheet, rod, tubing, and wire. One exception is Incoloy MA-956. Although this alloy might be fabricable in various forms, only information on sheet material is available. Similarly, nickel aluminides potentially can be fabricated into various shapes; however, the fabrication technology is not yet mature. Currently, properties are being obtained on cast and rolled sheet.

Weldability in the present context refers to the ability to join materials to themselves without causing significant degradation of physical and mechanical properties. As in the case of fabricability, all of the alloys except MA-956 and the nickel aluminides can be welded by well-established techniques. Welding of MA-956 causes redistribution of dispersoid particles and an attendant degradation of mechanical properties.

In the case of nickel aluminides, cracks in the welds have been a problem. Welding also affects the long-range atomic order that had previously been established by selected heat treatments. As a result, some degradation of mechanical properties occurs. Restoring the properties by heat treatment of large assemblies might be difficult.

Although specifications for creep strength, rupture life, and other mechanical properties might be required in designing a heat exchanger, the ultimate tensile strength (provided by the manufacturers) is used in this discussion. The ultimate tensile strength is shown at 600, 800, and 1000°C in Table 5. Projected annual corrosion rates, fabricability (availability in various shapes), and weldability are also shown in Table 5 to provide a comparison summary. Selection of a single material would involve compromises because none of the materials are clearly superior to the others in terms of all factors presented in Table 5. The combination of very low corrosion rate, good fabricability and weldability, and moderate strength make Alloy 214 a highly ranked candidate for applications in high-temperature, NaCl-containing atmospheres. Nickel aluminide IC-221, which is significantly stronger than the other alloys at 1000°C and had the second lowest corrosion rate, is another good candidate if fabrication and welding problems can be solved. Selection of one of the other alloys would probably impose a penalty in strength or corrosion rate.

Resistance to corrosion in a NaCl-containing atmosphere does not imply resistance to other atmospheres. For example, Ni-base alloys are susceptible to severe corrosion in atmospheres containing sulfur because of formation of various nickel sulfides.<sup>7</sup> These sulfides can cause formation of liquid phases at or below typical heat exchanger temperatures. In fact, a Ni-Ni<sub>3</sub>S<sub>2</sub> eutectic occurs at 645°C. Liquid phases destroy the protective oxide layers on alloys and cause catastrophic corrosion. Iron-base alloys have better resistance to sulfur than Ni-base alloys. Laboratory tests of various alloys in a simulated fluidized-bed combustor atmosphere demonstrated the poor performance of Ni-base alloys.<sup>8</sup> Austenitic stainless with 8 to 22% Ni (types 304, 316 and 310) exhibited substantially less corrosion than Incoloy 800 (~31% Ni), Haynes 188 (~22% Ni and ~38% Co), and RA-330 (~35% Ni). Nickel aluminide IC-50 developed a nickel sulfide phase,

Table 5. Characteristics of alloys

| Alloy                      | Ultimate tensile strength <sup>a</sup><br>(MPa) |       |        | Corrosion rate <sup>b</sup> |          | Available shapes    | Weldable        |
|----------------------------|---|-------|--------|-----------------------------|----------|---------------------|-----------------|
|                            | 600°C   | 800°C | 1000°C | mm/year                     | in./year |                     |                 |
| Incoloy MA-956             | 275   | 140   | 100    | 4.1                         | 0.16     | Sheet               | No <sup>c</sup> |
| Incoloy 800                | 475   | 180   | 55     | 4.4                         | 0.17     | Standard mill forms | Yes             |
| Inconel 625                | 895   | 450   | 140    | 3.6                         | 0.14     | Standard mill forms | Yes             |
| Inconel 601                | 550   | 200   | 70     | 2.9                         | 0.11     | Standard mill forms | Yes             |
| Alloy 214                  | 690   | 525   | 120    | 0.3                         | 0.01     | Standard mill forms | Yes             |
| Hastelloy X                | 605   | 405   | 155    | >2.2                        | >0.08    | Standard mill forms | Yes             |
| Haynes 188                 | 730   | 570   | 230    | 9.3                         | 0.37     | Standard mill forms | Yes             |
| Nickel aluminide<br>IC-50  | 735   | 550   | 275    | >2.9                        | >0.12    | Standard mill forms | No <sup>d</sup> |
| Nickel aluminide<br>IC-221 | 1190  | 930   | 370    | 0.8                         | 0.03     | Sheet               | No <sup>d</sup> |

<sup>a</sup>From manufacturers' data in the case of commercial alloys; private communication from C. T. Liu (ORNL) in the case of nickel aluminides.

<sup>b</sup>In oxidizing atmosphere containing NaCl at 1000°C. Rates projected from data in Table 4.

<sup>c</sup>Welding causes redistribution of dispersoid and loss of strength.

<sup>d</sup>Welding procedures are not yet established.

which would eventually cause severe attack, whereas Fe-base aluminides formed more protective (Fe, Al) oxides.

Selection of materials for heat exchanger applications, therefore, require an assessment of corrosion behavior, mechanical properties, fabricability, and weldability. The selected material will probably represent a compromise among these factors.

#### ACKNOWLEDGMENTS

The contributions of other persons to this work are gratefully acknowledged: P. J. Jones, specimen preparation and corrosion testing; J. R. Mayotte, metallographic preparation and measurements; E. L. Long, Jr., and C. T. Liu, technical review of the draft; A. J. Moorhead, helpful discussions; F. W. Christie, preparation of the draft; and D. L. Balltrip, final preparation of the report.

#### REFERENCES

1. J. E. Snyder and D. R. Petrak, "Design and Materials Selection for a High-Temperature Burner-Duct Recuperator," pp. 59-77 in *Advances in Ceramics, Vol. 14, Ceramics in Heat Exchangers*, eds. B. D. Foster and J. B. Patton, The American Ceramic Society, Columbus, Ohio, 1985.
2. M. Coombs, D. Kotchick, and H. Strumpf, "A High-Temperature Ceramic Recuperator for Industrial Applications," pp. 49-50 in *Advances in Ceramics, Vol. 14, Ceramics in Heat Exchangers*, eds. B. D. Foster and J. B. Patton, The American Ceramic Society, Columbus, Ohio, 1985.
3. A. H. Kreeger, "Fluid Bed Waste Heat Boiler Operating Experience in Dirty Gas Streams," pp. 37-42 in *Vol. I, Proceedings of the Eighth Annual Industrial Energy Technology Conference and Exhibition*, Houston, Texas, June 17-19, 1986.
4. K. D. Patch, W. E. Cole, and M. A. Shimko, *Full-Scale Design of a Fluidized-Bed Waste-Heat Recovery System*, DOE/ID/12302-8, Thermo Electron Corporation, Waltham, Massachusetts, January 30, 1987.

5. J. I. Federer and P. J. Jones, *Oxidation/Corrosion of Metallic and Ceramic Materials in an Aluminum Remelt Furnace*, ORNL/TM-9741, December 1985.

6. J. I. Federer, *An Investigation of Ceramic Coatings for Protection of SiC from High-Temperature Corrosion*, ORNL/TM-10606, February 1988.

7. M. Hansen, *Constitution of Binary Alloys*, McGraw-Hill Book Company, Inc., New York, 1958, p. 1034.

8. K. Natesan and W. Podolski, *Atmospheric Fluidized-Bed Cogeneration Air Heater Experiment: 1000-h Laboratory Test A*, ANL-87-11, Argonne National Laboratory, Argonne, Illinois, 1987.

## INTERNAL DISTRIBUTION

- |        |                               |     |                                 |
|--------|-------------------------------|-----|---------------------------------|
| 1-2.   | Central Research Library      | 29. | C. T. Liu                       |
| 3.     | Document Reference Section    | 30. | E. L. Long, Jr.                 |
| 4-5.   | Laboratory Records Department | 31. | A. J. Moorhead                  |
| 6.     | Laboratory Records, ORNL RC   | 32. | O. O. Omatete                   |
| 7.     | ORNL Patent Section           | 33. | A. C. Schaffhauser              |
| 8-10.  | M&C Records Office            | 34. | M. A. Schmidt                   |
| 11.    | R. W. Barnes                  | 35. | V. K. Sikka                     |
| 12.    | T. M. Besmann                 | 36. | G. M. Slaughter                 |
| 13.    | P. J. Blau                    | 37. | D. P. Stinton                   |
| 14.    | R. A. Bradley                 | 38. | R. W. Swindeman                 |
| 15.    | R. S. Carlsmith               | 39. | V. J. Tennery                   |
| 16.    | D. F. Craig                   | 40. | J. R. Weir, Jr.                 |
| 17.    | J. H. DeVan                   | 41. | D. F. Wilson                    |
| 18.    | J. R. DiStefano               | 42. | A. D. Brailsford, Consultant    |
| 19-23. | J. I. Federer                 | 43. | H. D. Brody, Consultant         |
| 24.    | J. R. Keiser                  | 44. | F. F. Lange, Consultant         |
| 25.    | H. E. Kim                     | 45. | D. Pope, Consultant             |
| 26.    | O. F. Kimball                 | 46. | E. R. Thompson, Consultant      |
| 27.    | J. F. King                    | 47. | J. B. Wachtman, Jr., Consultant |
| 28.    | W. Koncinski                  |     |                                 |

## EXTERNAL DISTRIBUTION

48. AIRESEARCH MANUFACTURING COMPANY, 2525 W. 190th Street, Torrance, CA 90509  
D. M. Kotchick
49. BABCOCK AND WILCOX, P.O. Box 239, Lynchburg, VA 24505  
W. P. Parks, Jr.
50. COMBUSTION ENGINEERING, INC., 911 West Main Street, Chattanooga, TN 37402  
C. H. Sump
51. CONSOLIDATED NATURAL GAS, 11001 Cedar Avenue, Cleveland, OH 44106  
J. Bjerklie

- 52-54. COORS PORCELAIN COMPANY, 600 Ninth Street, Golden, CO 80501  
C. Dobos  
R. Kleiner  
D. Roy
- 55-56. GTE PRODUCTS CORPORATION, Hawes Street, Towanda, PA 18848  
J. L. Ferri  
J. Gonzalez
57. GAS RESEARCH INSTITUTE, 8600 W. Bryn Mawr Ave., Chicago, IL 60631  
R. Ruiz
58. HAGUE INTERNATIONAL, 3 Adam Street, South Portland, MA 04106  
S. B. Young
- 59-60. IDAHO NATIONAL ENGINEERING LABORATORY, P.O. Box 1625, Idaho Falls,  
ID 83415  
F. W. Childs  
M. S. Sohal
- 61-62. NORTON COMPANY, Worcester, MA 01606  
B. D. Foster  
M. L. Torti
63. PENNSYLVANIA STATE UNIVERSITY, 201 Steidle Building, University  
Park, PA 16801  
R. E. Tressler
- 64-65. SOLAR TURBINES INCORPORATED, P.O. Box 8537, San Diego, CA  
92138-5376  
M. E. Ward  
M. Van Roode
66. STONE & WEBSTER ENGINEERING CORPORATION, P.O. Box 2325, Boston,  
MA 02107  
P. E. Koppel
- 67-69. TECOGEN, INC., P.O. Box 9046, Waltham, MA 02254-9046  
W. E. Cole  
K. D. Patch  
S. R. Wysk
70. UNIVERSITY OF ILLINOIS AT CHICAGO, P.O. Box 4348, Chicago,  
IL 60680  
M. J. McNallan

- 71. DOE, IDAHO OPERATIONS OFFICE, 550 Second Street, Idaho Falls,  
ID 83401  
G. R. Peterson
- 72. DOE, MORGANTOWN ENERGY TECHNOLOGY CENTER, P.O. Box 880,  
Morgantown, WV 26505  
J. M. Hobday
- 73. DOE, OAK RIDGE OPERATIONS OFFICE, P.O. Box 2001, Oak Ridge, TN  
37831-8600  
Office of Assistant Manager for Energy Research and  
Development
- 74-76. DOE, OFFICE OF INDUSTRIAL CONSERVATION, 1000 Independence Ave.,  
Forrestal Building, Washington, DC 20585  
J. Eustis  
S. L. Richlen  
J. R. Rossmeissl
- 77-86. DOE, OFFICE OF SCIENTIFIC AND TECHNICAL INFORMATION, Office of  
Information Services, P.O. Box 62, Oak Ridge, TN 37831  
For distribution by microfiche as shown in DOE/TIC-4500,  
Distribution Category UC-95 (Energy Conservation)